

Electronic Supplementary Information

Probing into Dimension and Shape Control Mechanism of Copper(I) Sulfide Nanomaterials via Solventless Thermolysis Based on Mesogenic Thiolate Precursors

Junfei Duan, Liang Liu, Zhongying Wu, Jianglin Fang,* and Dongzhong Chen*

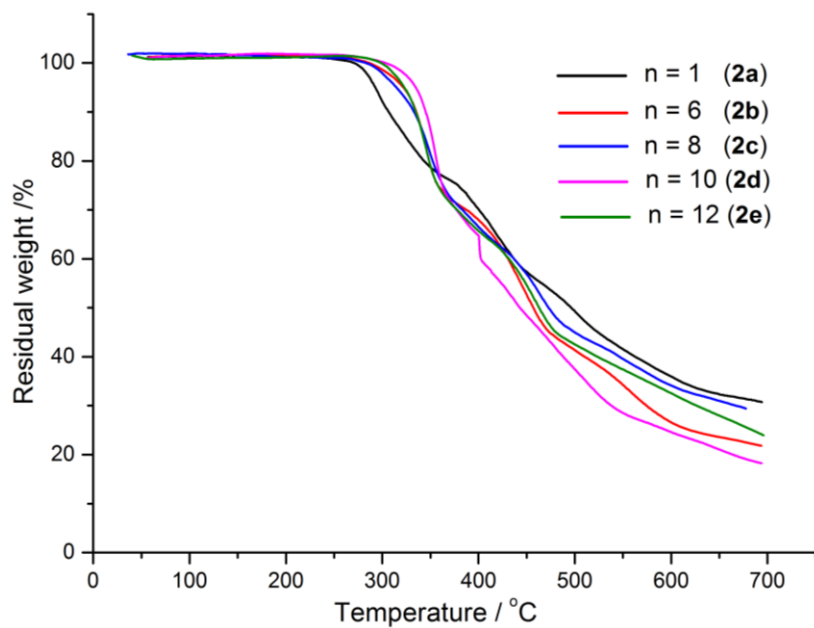


Figure S1. TGA thermograms of the series copper thiolates **2** with variant length alkyloxy tails.

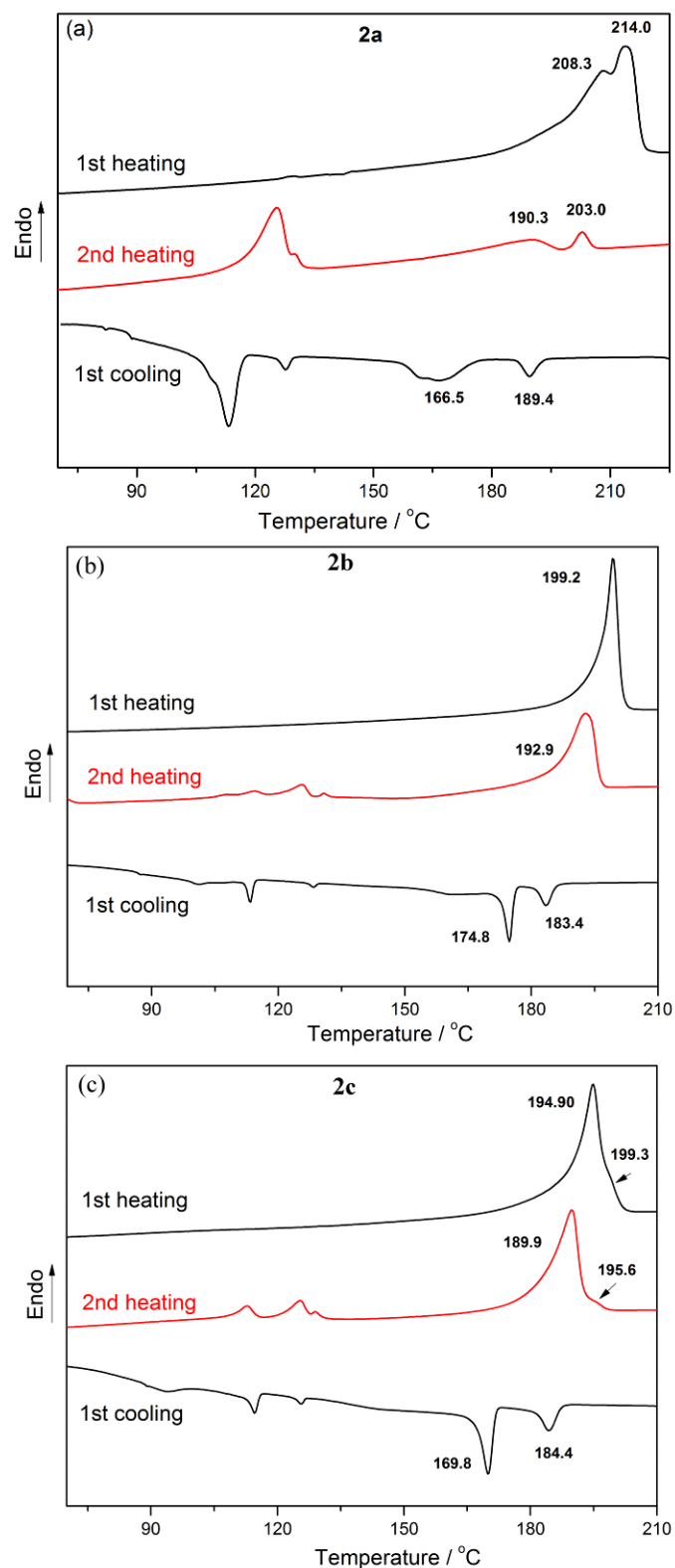


Figure S2. DSC thermograms of the series copper thiolates during the 1st heating and cooling, and 2nd heating scans at a rate of 20 °C/min for (a) **2a**; (b) **2b**, and (c) **2c**.

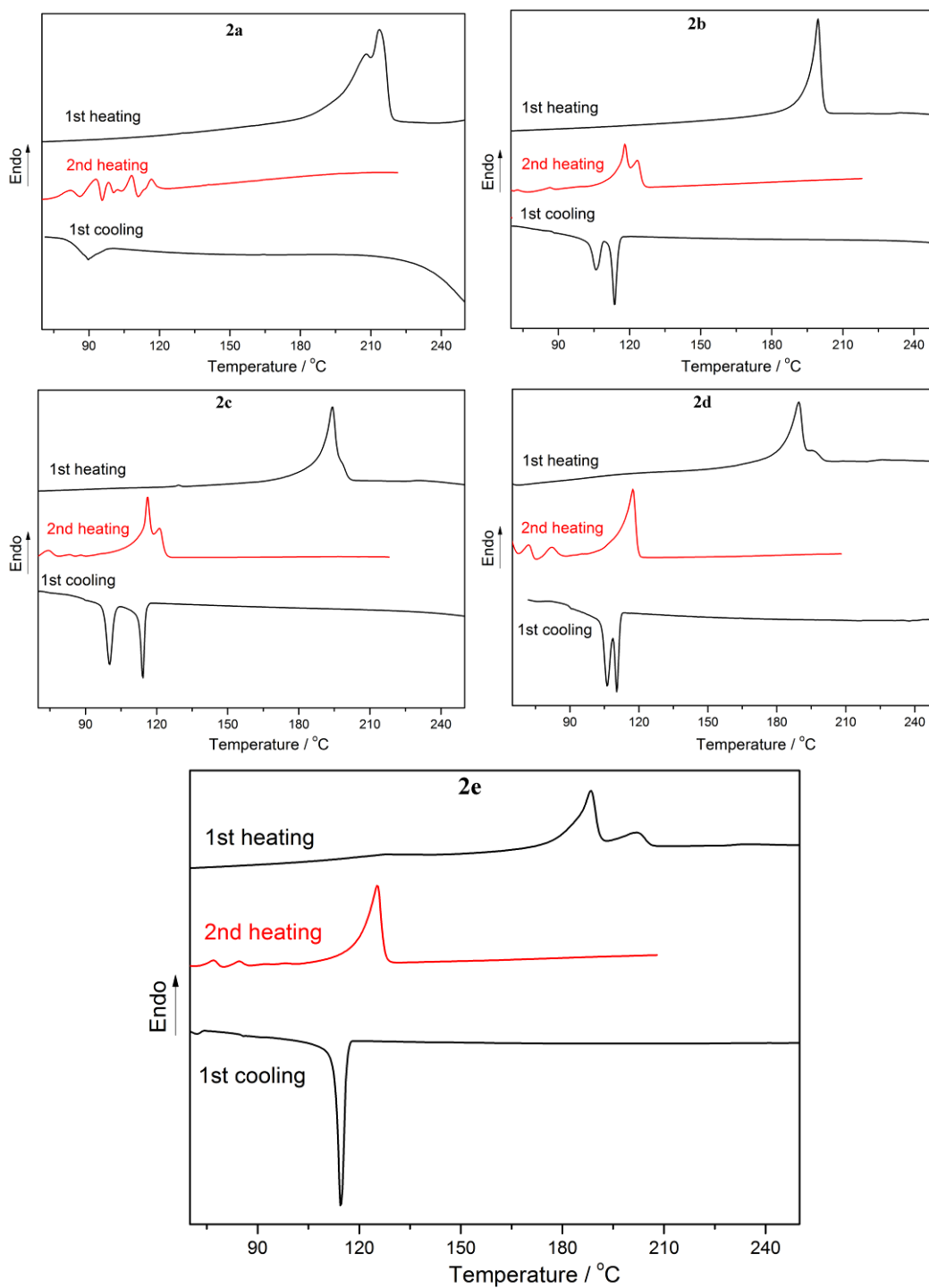


Figure S3. DSC thermograms of the series copper thiolates from **2a** to **2e** upon heating or cooling in the temperature range of 70-250 °C (1st thermal cycles) and 70-210 °C (2nd heating run) at a slow rate of 2 °C/min.

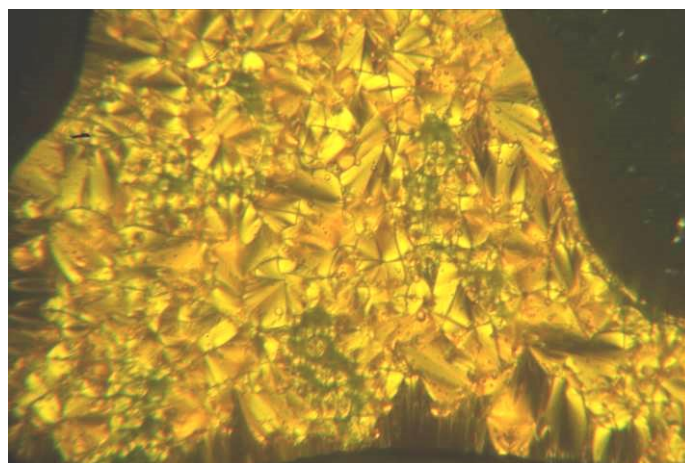


Figure S4. Typical focal conic POM texture under crossed polarizers of mesogenic azobenzene thiol ligand **1d** at 95 °C showing a monotropic smectic A phase.

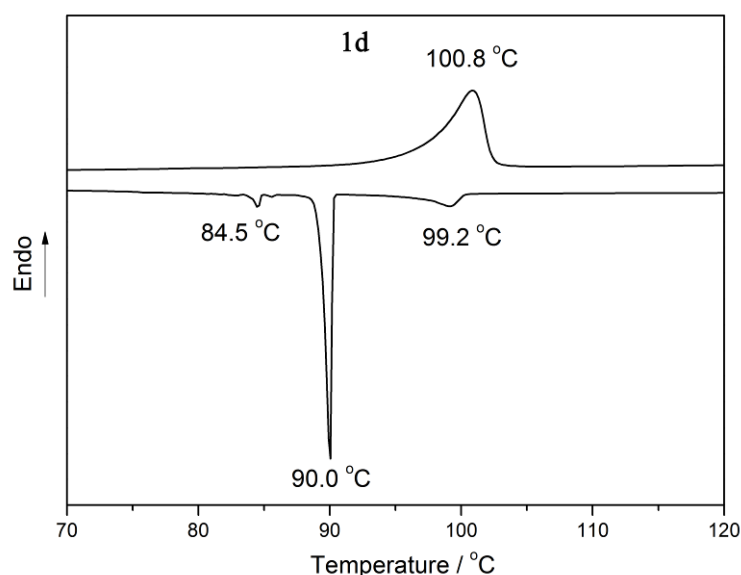


Figure S5. DSC thermograms of mesogenic azobenzene thiol ligand **1d** during the 1st cooling and 2nd heating scans in the temperature range of 70 ~120 °C at 20 °C min⁻¹, manifesting a monotropic LC mesophase upon cooling.

Table S1. Thermal properties and phase assignments for azobenzene thiol ligand **1d** from the first cooling and second heating runs

code	T_{decomp} (°C) ^{a)}	Thermal cycle	Transition T/°C [ΔH (J g ⁻¹) ^{b),c)}	LC range (°C)
1d	241	cooling	I 99.2 [8.4] SmA 90.0 [78.0] Cr ₁ 84.5 [2.8] Cr ₂	9
		heating	Cr 100.8 [111.9] I	/

^{a)} The onset of decomposition temperature determined from TGA at a heating rate of 20 °C min⁻¹ under nitrogen atmosphere; ^{b)} The phase transition temperatures and enthalpy changes (in square brackets) obtained from DSC at 20 °C min⁻¹; ^{c)} Abbreviations: Cr = crystalline, SmA = smectic A, I = isotropic;

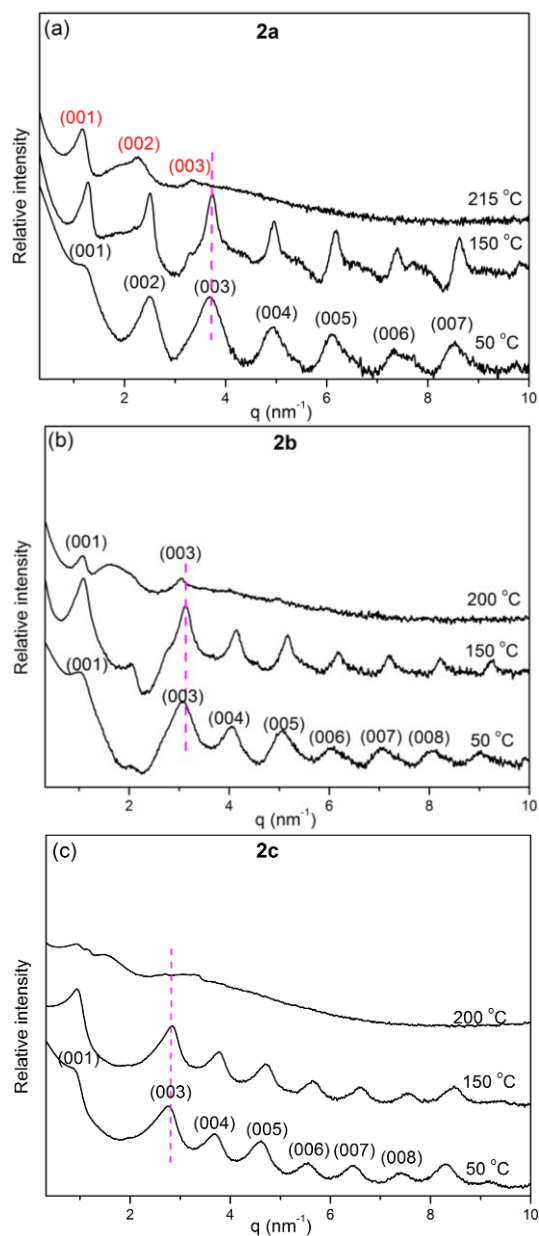


Figure S6. Variable-temperature SAXS/WAXS profiles of the series copper thiolates **2a**, **2b**, and **2c**. Some broad bands coexisted with layered reflections were presumably attributed to the mixture of residual layered structure of precursors and some products formed due to partial thermolysis within the time period of measurement when the temperature heating close to isotropic phase for **2b** and **2c**; while mainly copper(I) sulfide nanoparticles constrained in the layered structure were achieved (with spacing indexing in red color), manifesting a deeper degree of thermolysis for **2a** upon heating to 215 °C.

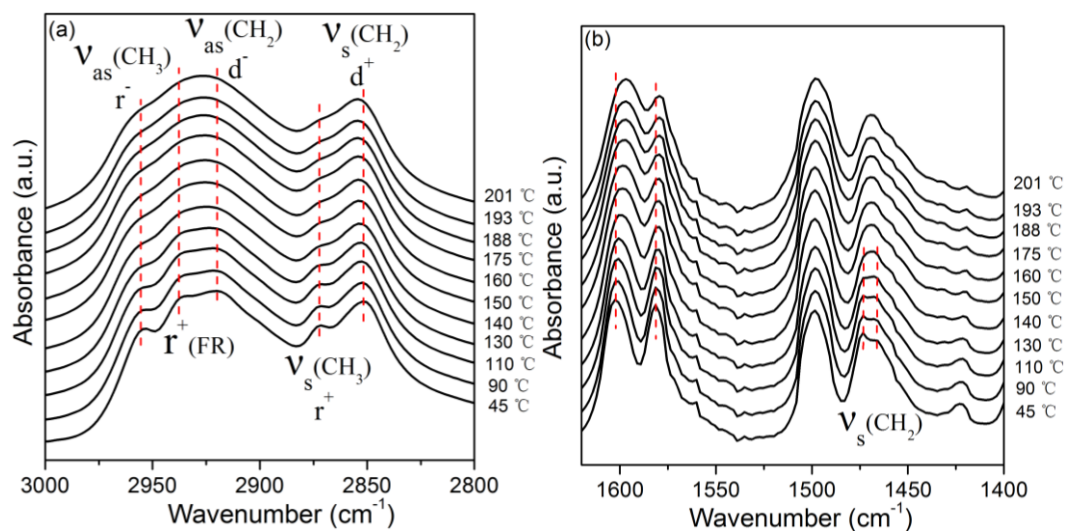


Figure S7. Variable-temperature FTIR spectra of **2d** over the temperature range 30–201 °C at (a) high-frequency region 3000–2800 cm^{-1} ; and (b) middle-frequency region 1650–1400 cm^{-1} .

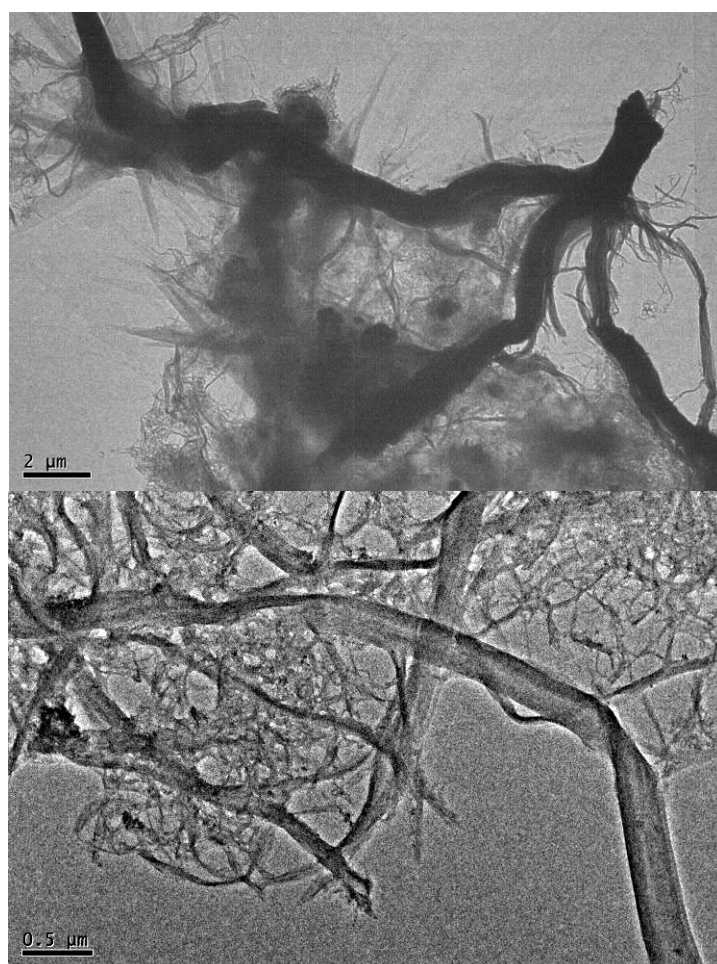


Figure S8. TEM images of ultrathin Cu_2S nanowire bundles in the large-scale range produced from **2d** annealing at 200 °C for 1 h under vacuum.

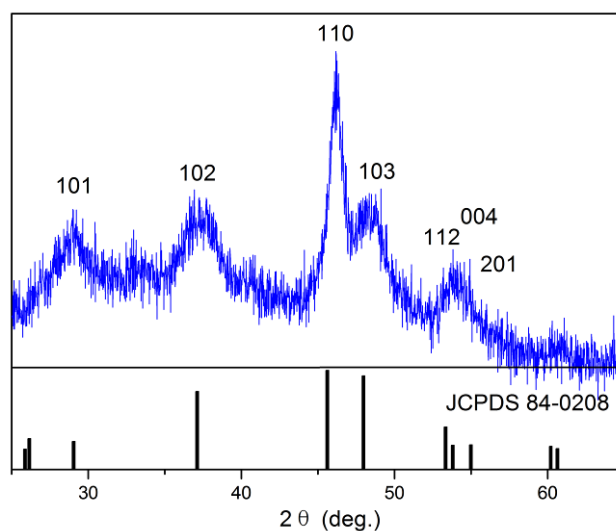


Figure S9. Comparison of XRD profile of Cu₂S nanowires produced from **2d** at 200 °C for 1 h under vacuum with the (chalcocite) Cu₂S hexagonal-phase pattern of standard card #JCPDS 84-0208.

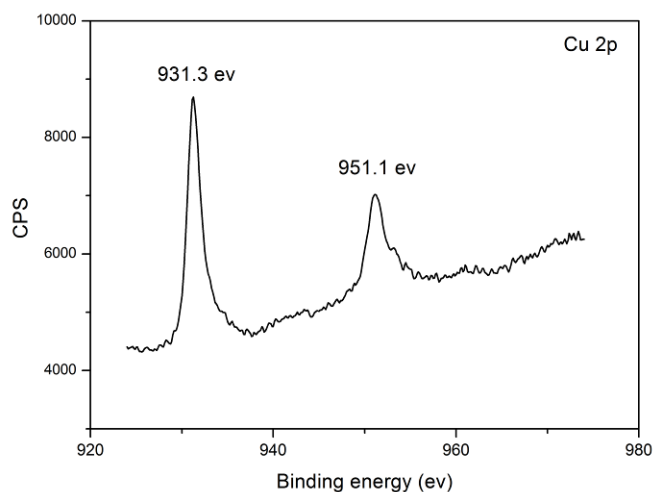


Figure S10. Representative XPS profiles of Cu2p region of Cu₂S nanowires produced from **2d** at 200 °C for 1 h under vacuum.

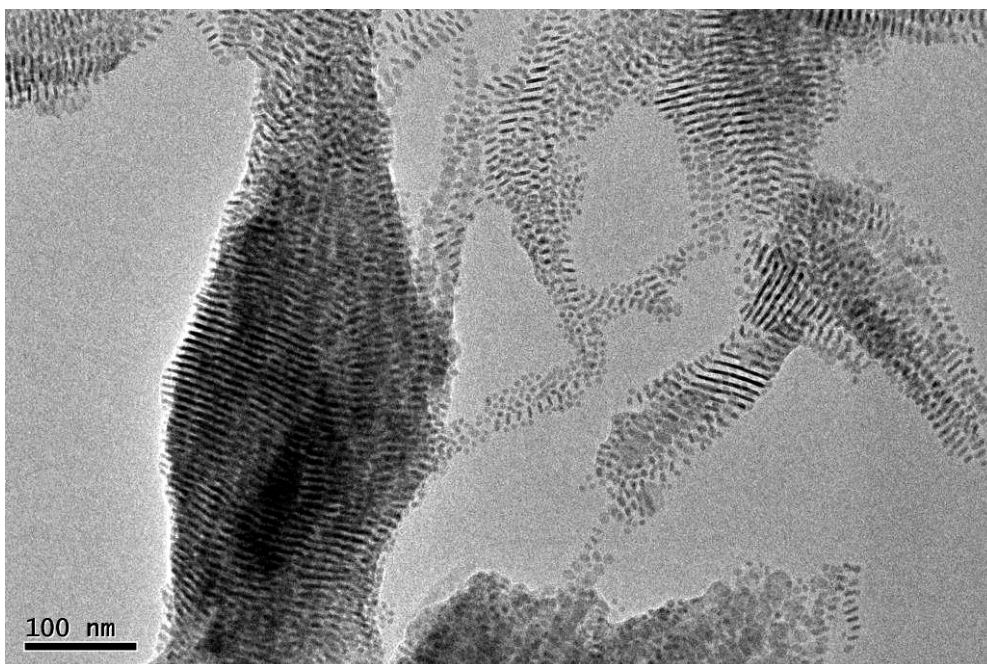


Figure S11. TEM images of self-assembled Cu₂S nanorods (with signs of partially formation of nascent nanodisks) produced from **2d** annealing at 240 °C for 0.5 h under vacuum.

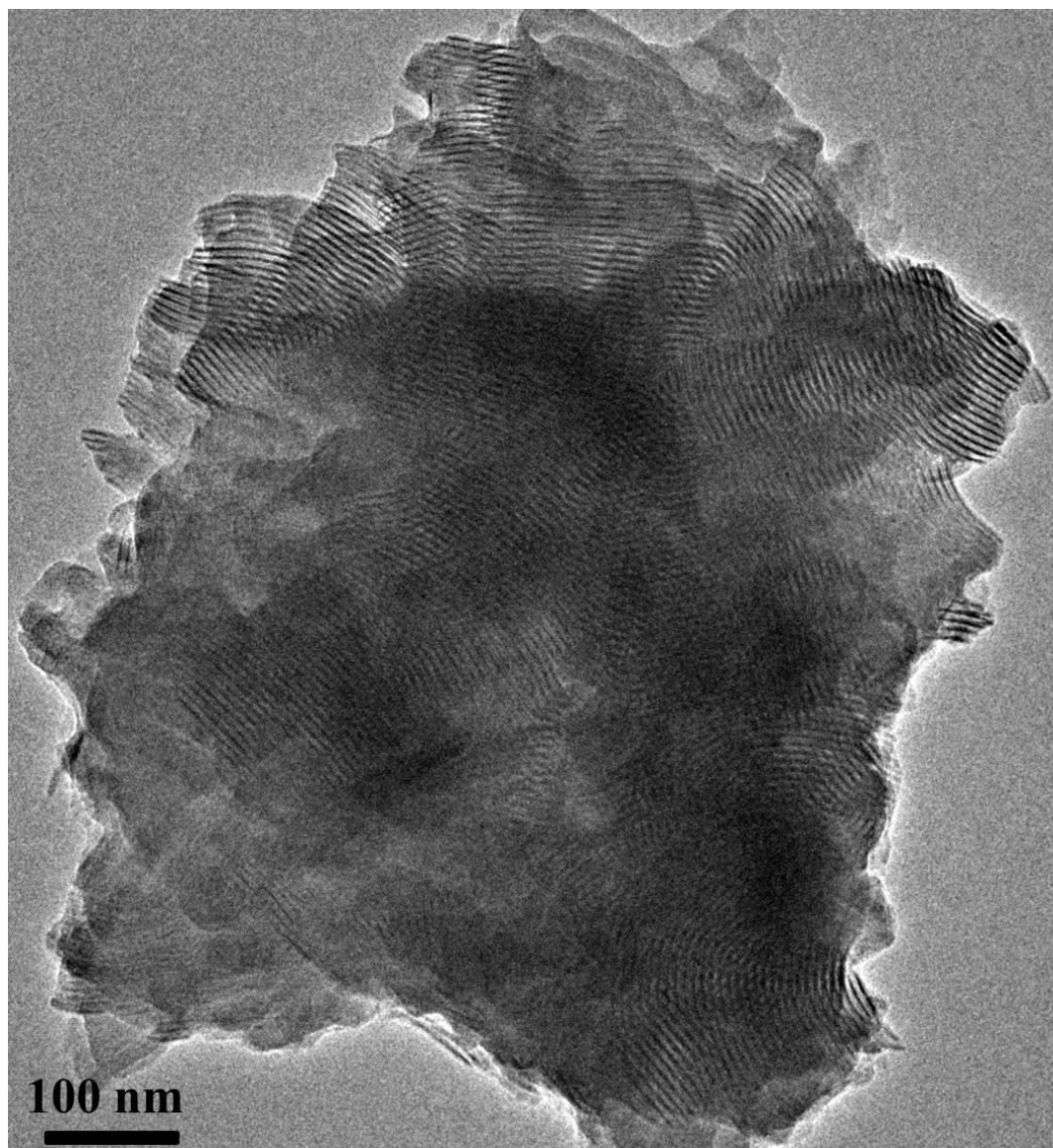


Figure S12. TEM images of ultrathin Cu_2S nanowires produced from **2d** annealing at $220\text{ }^\circ\text{C}$ for 1 h under vacuum.

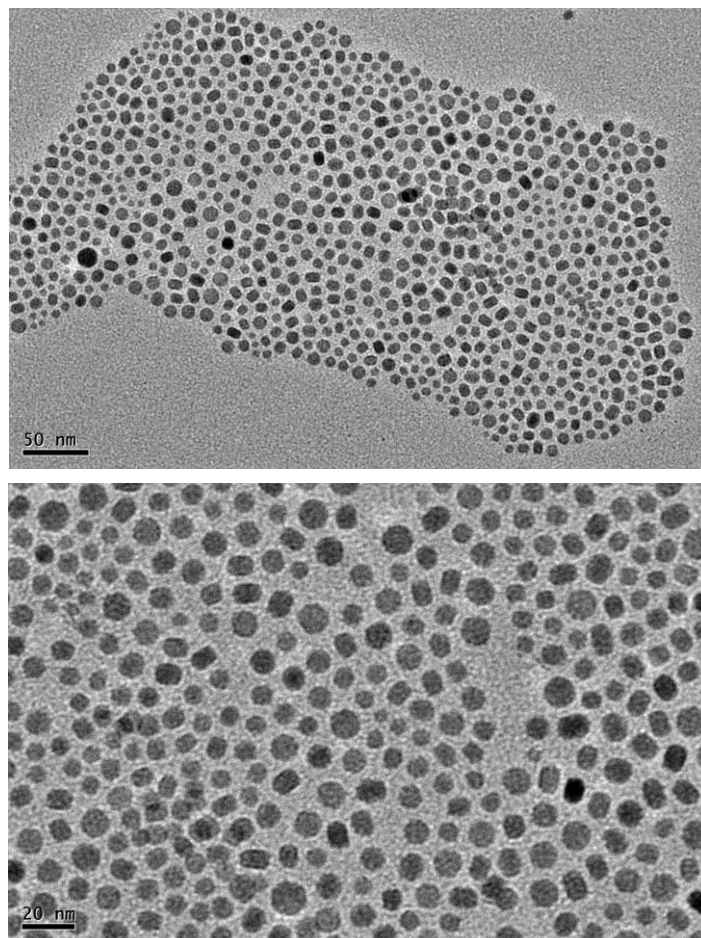


Figure S13. TEM images of Cu_2S nanodisks produced from **2d** annealing at 220 °C for 1 h under argon atmosphere.

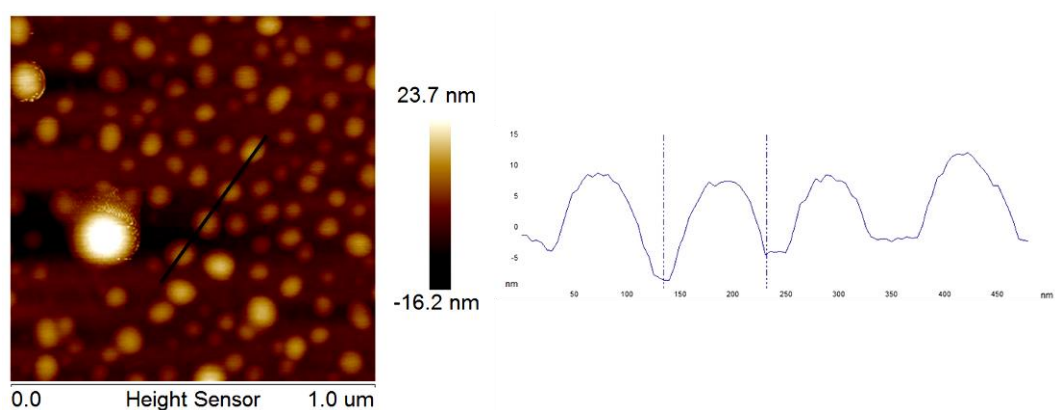


Figure S14. (left) AFM images of the Cu_2S nanodisks produced from the thiolate **2d** thermolytic reaction at 220 °C for 1 h under argon atmosphere, and (right) the height profiles along the line labeled in the left Figure. The height is around 10.0 nm.

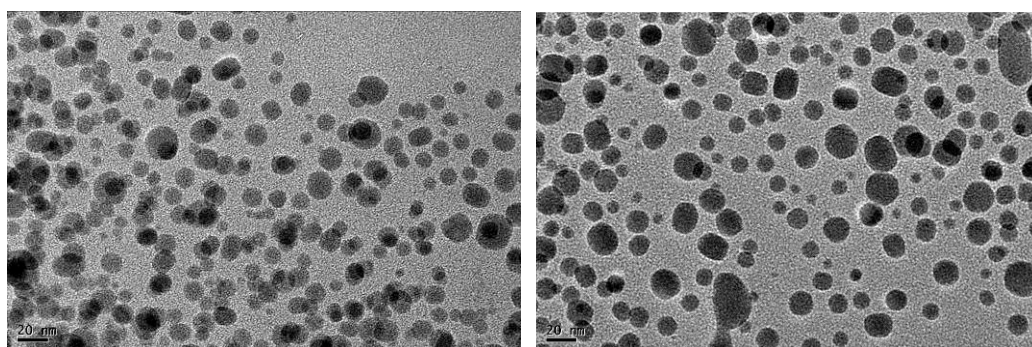
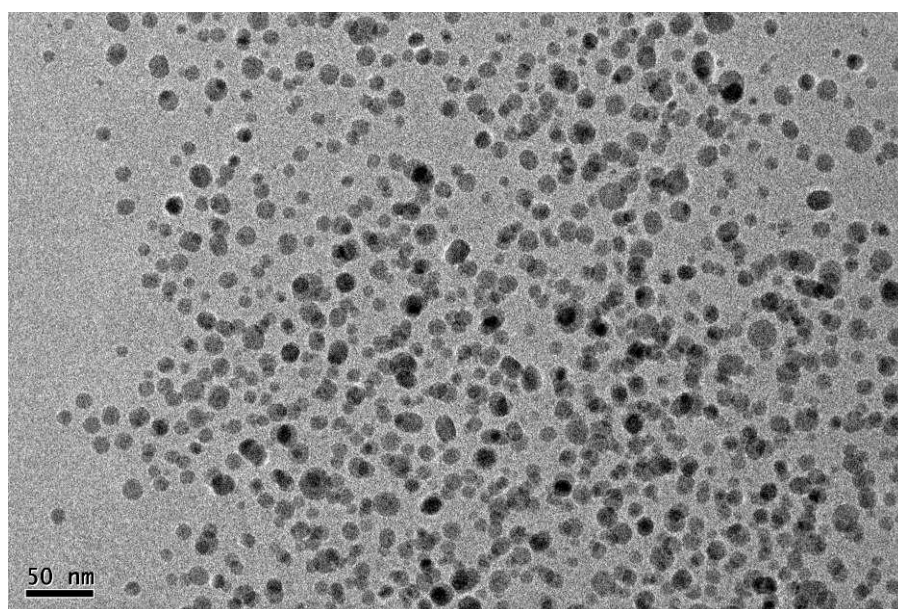
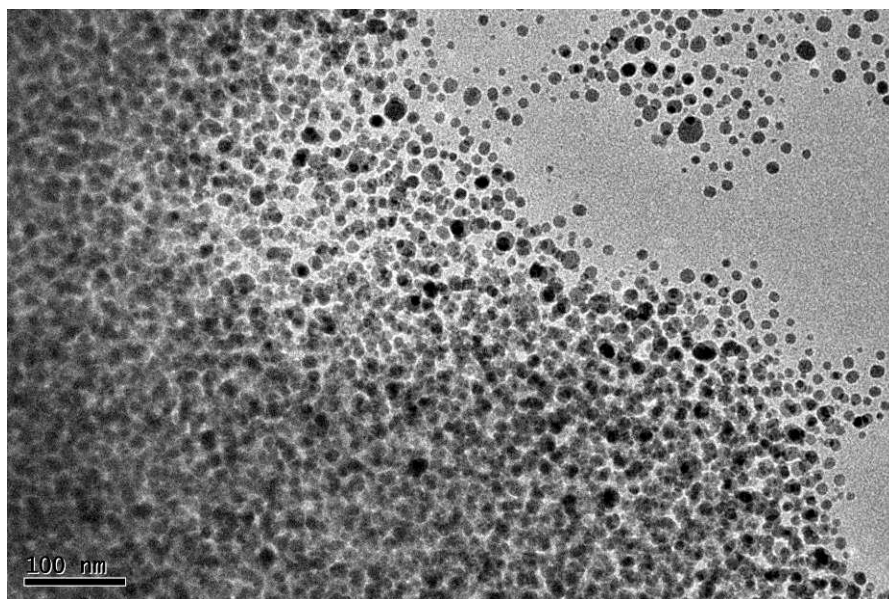


Figure S15. TEM images of dispersed irregular Cu₂S nanodisks and spherical nanoparticles produced from **2d** annealing at 240 °C for 1 h under argon atmosphere.

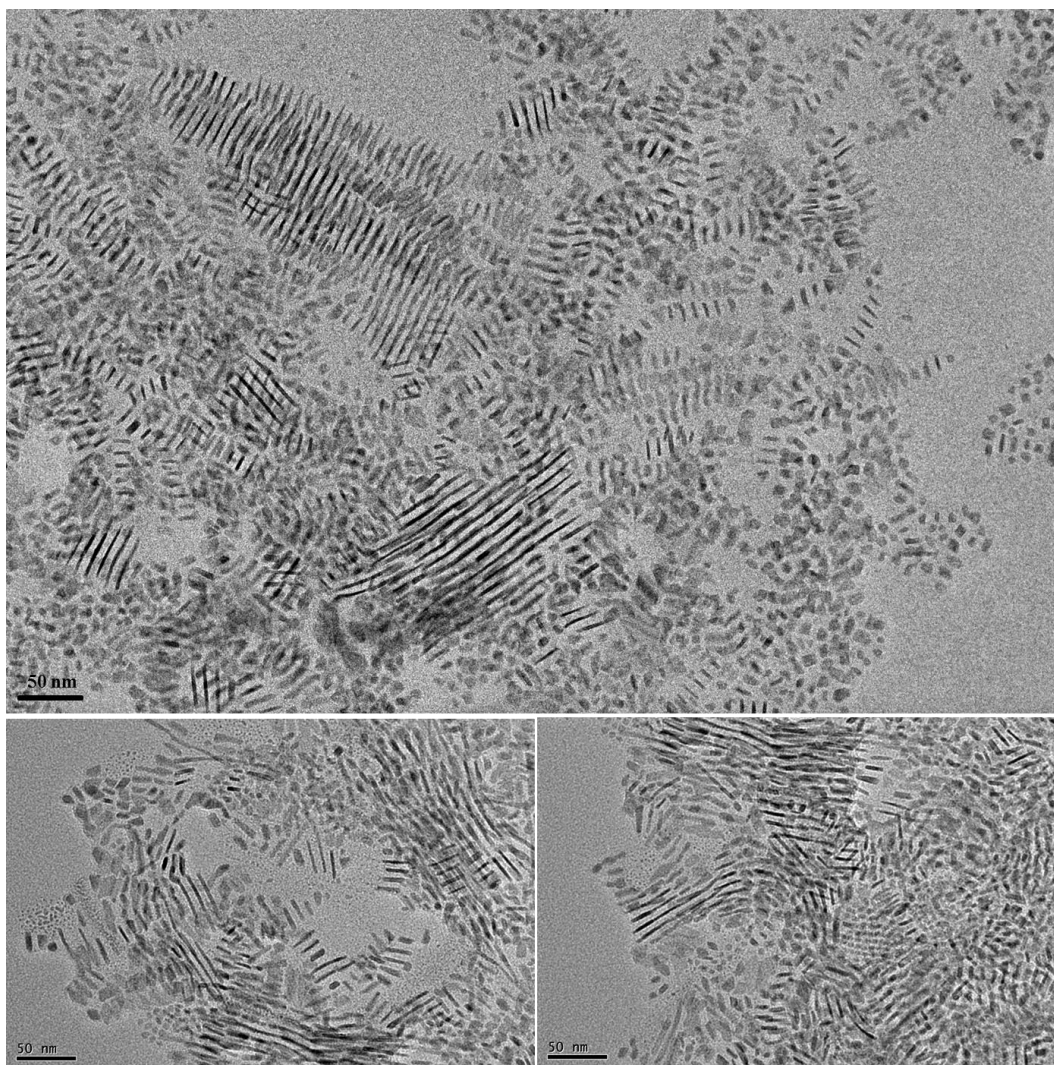


Figure S16. TEM images of mixed Cu₂S nanowires, nanorods and preliminary nanodisks produced from **2d** annealing at 200 °C for 0.5 h under air.

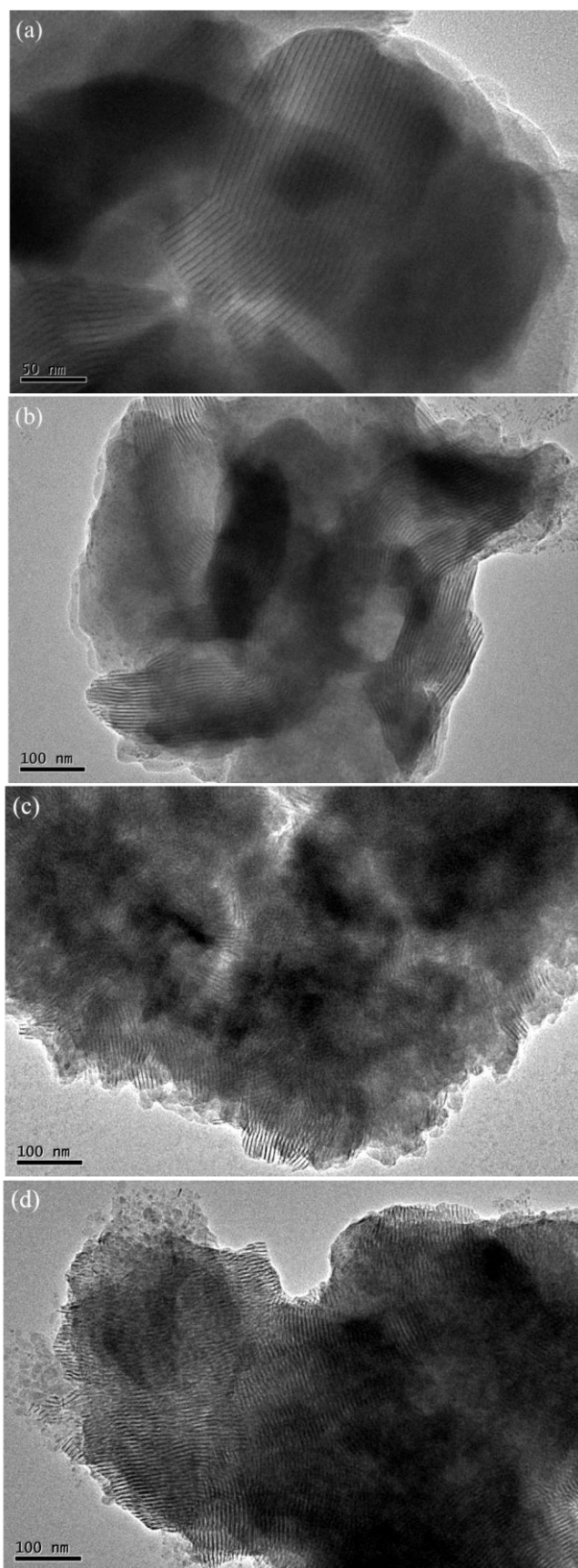


Figure S17. TEM images of self-assemble Cu_2S nanowires produced from (a) **2a**, (b) **2b**, (c) **2c**, (d) **2e**, annealing at 215 °C (for **2a**) or 200 °C (for **2b**, **2c** and **2e**) for 1 h under vacuum.

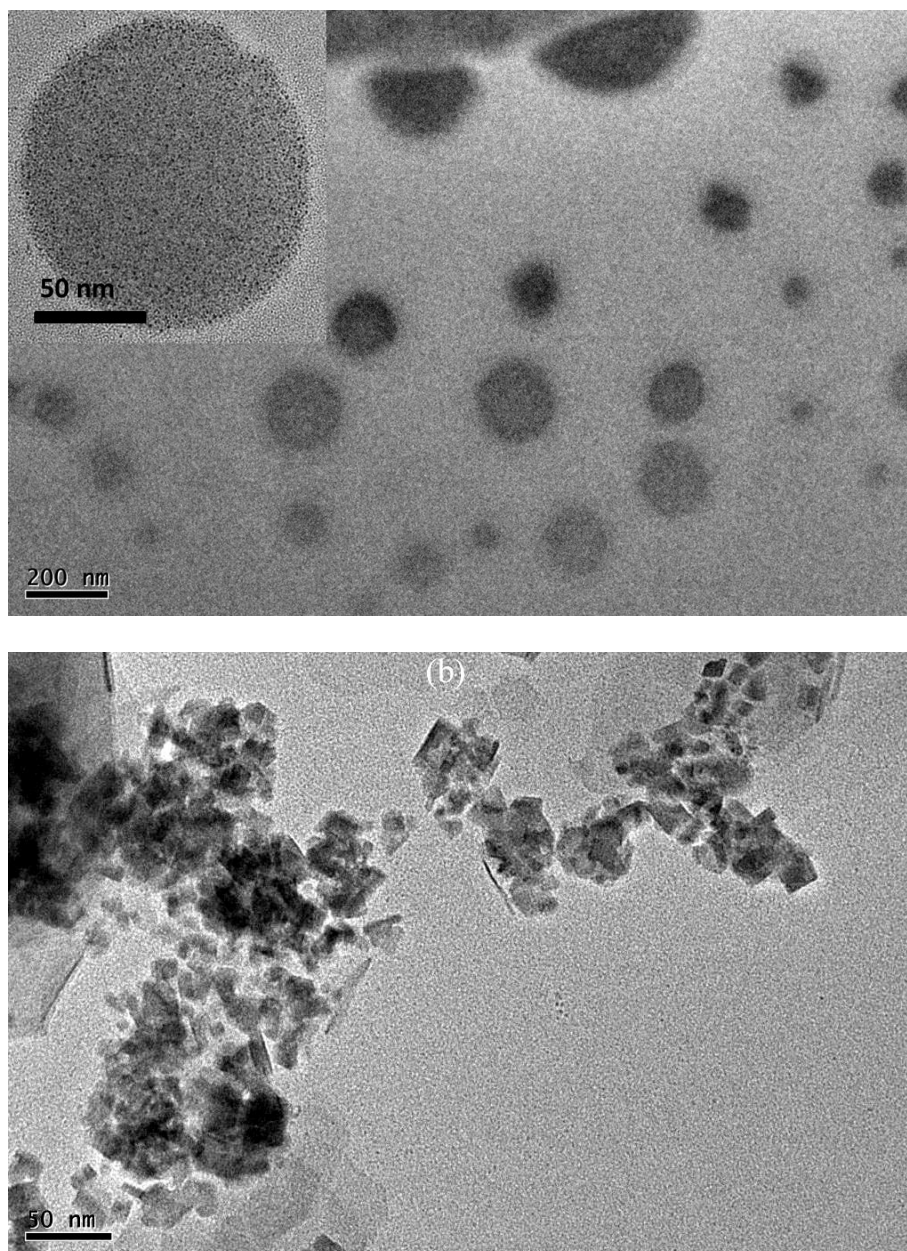


Figure S18. TEM images of Cu_2S nanocrystals produced from **2a** (a) annealing at 220 °C for 1h under vacuum, (b) annealing at 220 °C for 1h under argon atmosphere.

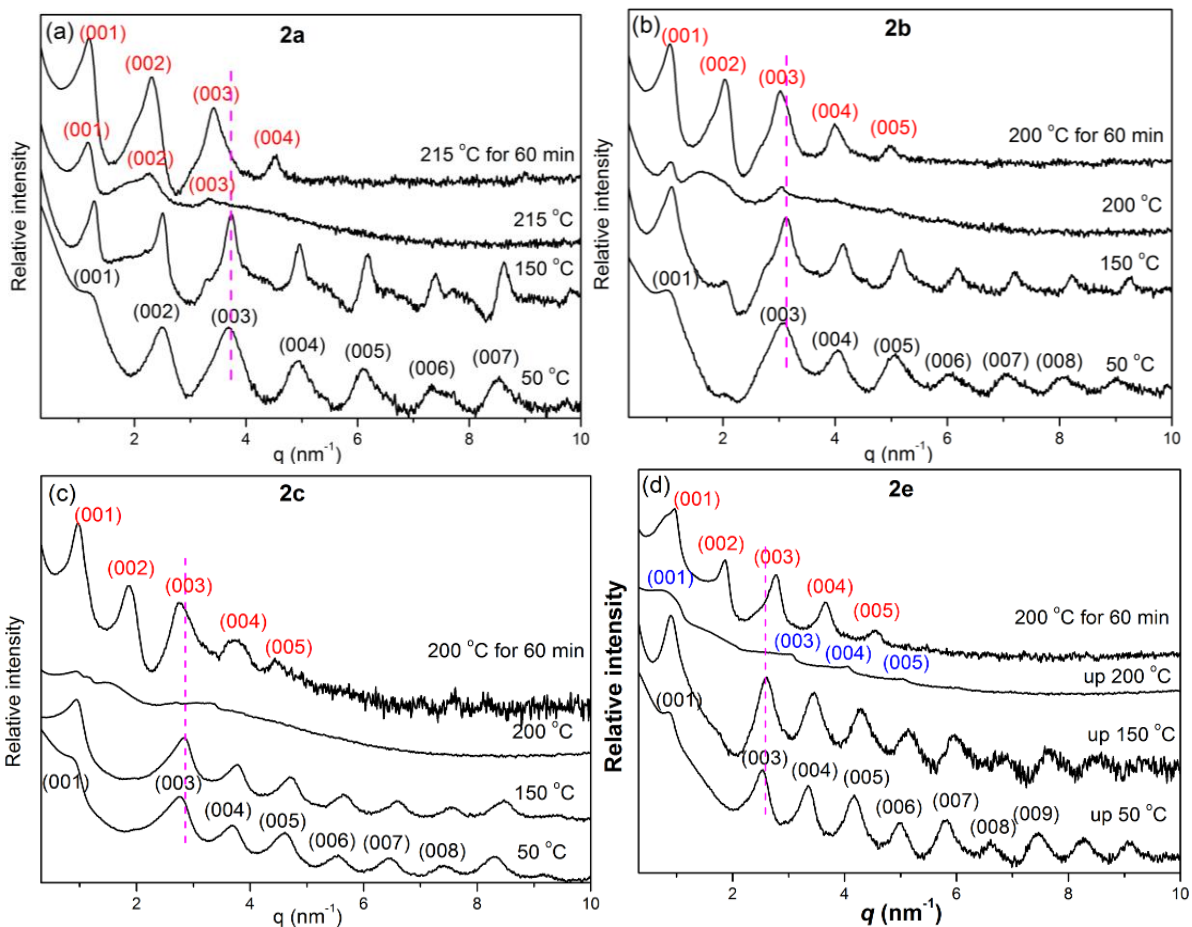


Figure S19. SAXS/WAXS profiles of copper thiolate **2a-2c** and **2e** at variant temperatures and self-assembled Cu₂S nanowires produced after annealing at 215 °C (for **2a**) or 200 °C (for **2b**, **2c**, and **2e**) for 1 h.